Journal of Power Sources 556 (2023) 232396

Contents lists available at ScienceDirect

Journal of Power Sources

journal homepage: www.elsevier.com/locate/jpowsour

On the oxidation of isopropanol on platinum single crystal electrodes. A detailed voltammetric and FTIR study

Dalila S. Mekazni, Rosa M. Arán-Ais, Enrique Herrero, Juan M. Feliu *

Instituto de Electroquímica, Universidad de Alicante, Apdo. 99, E-03080, Alicante, Spain

HIGHLIGHTS

- Isopropanol oxidation to acetone on Pt is facilitated by adsorbed OH.
- The rate determining step is the reaction between adsorbed OH and isopropanol.
- Acetone is adsorbed on Pt(100) and Pt(110), partially blocking the surface.
- Pt(100) is the only surface in which the C–C bond is cleaved during oxidation.

ARTICLE INFO

Keywords:
Isopropanol oxidation
Platinum single crystal electrodes
Acetone
Kinetic measurements
OH adsorption

ABSTRACT

Isopropanol oxidation is studied on platinum single crystals using electrochemical techniques and FTIR spectroscopy at different isopropanol concentrations. Isopropanol oxidation is found to be facilitated by the presence of adsorbed OH on the electrode surface, which reacts with an isopropanol molecule to yield the adsorbed alkoxide. Thus, when sulfuric acid is used as the supporting electrolyte instead of perchloric acid, oxidation currents diminish drastically since sulfate hinders OH adsorption. Kinetic measurements reveal that the chemical reaction between adsorbed OH and isopropanol is the rate-determining step in the mechanism. Voltammetric and FTIR experiments show that acetone is the major product of the reaction. On the Pt(111) surface, acetone is produced exclusively, and oxidation currents are controlled by diffusion since, on this electrode, acetone is not adsorbed and the adsorbed OH mobility is high. The adsorption of acetone-related species on the Pt(110) surface, which partially block the surface, leads to slightly lower currents. On the other hand, the Pt(100) electrode is the one showing significant rates for the C–C bond cleavage, yielding adsorbed CO and other species. Although this route is a minor path, the surface blockage by these species leads to a significant diminution of the currents.

1. Introduction

Hydrogen is considered the next energy vector because it can lead the transition from an energy system based on fossil fuels to one that relies on renewable sources. Hydrogen can be easily generated in electrolyzers powered by renewable energy sources and the energy chemically stored in hydrogen can be transformed back into electricity in fuel cells. This strategy presents some problems: first, hydrogen, being a gas, has a low volumetric energy density, and, secondly, it requires deploying a new distribution system as the one currently used for liquid fuels is not suitable for hydrogen. In addition, the ideal locations for renewable energy power plants are far away from the areas where the demand is highest, which calls for an effective and efficient transport system. An alternative for hydrogen transport has emerged in the form of liquid organic hydrogen carriers (LOHCs) [1]. In this approach, hydrogen is used to hydrogenate a compound. This hydrogenated compound is then transported as a liquid, employing the already existing fuel distribution network, and used to generate electricity where needed, regenerating the initial compound. In this strategy, the pair acetone/isopropanol can make excellent LOHCs. Acetone can be easily hydrogenated by chemical or electrochemical methods to isopropanol [2–4]. In turn, isopropanol can be selectively oxidized to acetone in fuel cells, releasing the stored energy [5].

By far, platinum is the best pure metal to electrooxidize isopropanol in acid media. It has been shown that this reaction is structure sensitive [6,7]. The reaction mainly yields acetone as the final product, although

* Corresponding author.
E-mail address: Juan.feliu@ua.es (J.M. Feliu).

https://doi.org/10.1016/j.jpowsour.2022.232396
Received 27 September 2022; Received in revised form 7 November 2022; Accepted 11 November 2022
Available online 24 November 2022

some other products can be detected, such as adsorbed CO and CO_2 [8–12]. This behavior is different from that observed for the other C3 alcohol, n-propanol, in which the product distribution is wider [6, 13–15]. The almost exclusive reduction of isopropanol to acetone makes it in the perfect candidate for LOCH. However, its use in practical applications requires high efficiency in the oxidation reaction (high currents at low overpotentials) and a negligible formation of side products. To achieve these goals, detailed knowledge of the mechanism is required. In the present manuscript, isopropanol oxidation in perchloric acid is studied on platinum single-crystal electrodes using electrochemical and FTIR experiments. The observed dependence of the oxidation reaction electrocatalysis with the surface structure and isopropanol concentration will serve to gain insight into the oxidation mechanism and guide the development of more efficient electrocatalysts.

2. Experimental

Platinum single-crystal electrodes were prepared according to Clavilier's method as described in Ref. [16]. Low index, namely Pt(111), Pt(110), and Pt(100), and stepped surfaces have been used. The stepped electrodes were those vicinal to (111) pole corresponding to the crystallographic zones [1 $\bar{1}$ 0] and [01$\bar{1}$]. The stepped surfaces of the [1 $\bar{1}$ 0] series are composed of (*n*-1) atom-wide (111) terraces separated by monoatomic (110) steps and their Miller indices are Pt (*n*,*n*,*n*-2). On the other hand, the surfaces in the [01 $\bar{1}$] zone have *n* atom-wide terraces separated by monoatomic (100) steps and the corresponding Miller indices are Pt (*n*+1,*n*-1,*n*-1). Prior to any experiment, the electrodes were flame-annealed, cooled down in a H_2 +Ar atmosphere, and transferred to the cell under the protection of a droplet of pure water in equilibrium with this gaseous mixture. It has been shown that this treatment leads to surfaces whose experimental topography agrees with the ideal structure [17]. Single crystal electrodes used in voltammetric experiments have a surface area between 0.03 and 0.045 cm^2, measured with an optical microscope, whereas the areas for electrodes used in the FTIR experiments are between 0.08 and 0.12 cm^2. For single crystal surfaces, the geometrical and the active area have the same values.

Electrochemical experiments were carried out in glass cells using a Pt wire and reversible hydrogen electrode (RHE) as counter and reference electrodes, respectively. Cyclic voltammograms were recorded using an Autolab PGSTAT302 N potentiostat in a hanging meniscus configuration. The working solution was prepared using ultrapure water (Purelab flex, 18.2 MΩ) containing concentrated perchloric acid (Merck, for analysis) or sulfuric acid (Merck, Suprapur) as supporting electrolytes, and 2-propanol (Honeywell, ≥99,9%) in different concentrations.

In situ infrared reflection absorption spectroscopy (IRRAS) experiments were carried out with a Nicolet iS50 FTIR spectrometer equipped with a narrow-band DC-coupled MCT-A detector. The spectroelectrochemical cell had a prismatic CaF_2 window beveled at 60°. The experiments were carried out at room temperature. A reversible hydrogen electrode (RHE) and a gold wire were used as reference and counter electrodes, respectively. The IR spectra were collected with p-polarized light with a resolution of 8 cm^{-1} and are the average of over 100 interferograms. The spectra are presented as the ratio -log(R_2/R_1), where R_2 and R_1 are the reflectance values corresponding to the single beam spectra recorded at the sample and reference potentials, respectively. In this way, positive bands in the spectra are due to species formed or whose concentration has increased at the sampling potential with respect to the reference potential, whereas negative bands are associated with a diminution of the concentration of the species. Bipolar bands are found for adsorbed species that are present at the reference and the sampling potential and whose frequency is dependent on the electrode potential (Stark effect).

3. Results and discussion

3.1. Voltammetric behavior of the isopropanol oxidation reaction

The oxidation behavior of alcohols is strongly dependent on the surface structure of the platinum surface and also on the supporting electrolyte composition [18]. To get insight into the oxidation process,

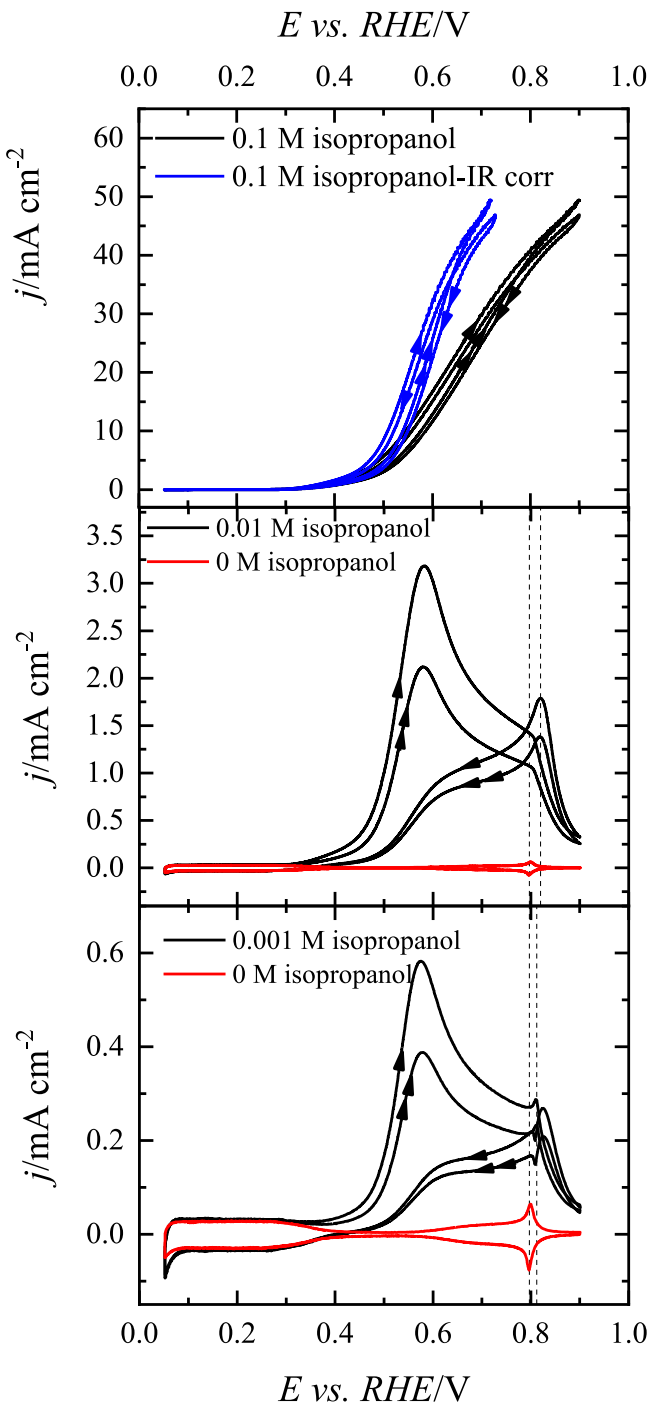

Fig. 1. Voltammetric profiles for the Pt(111) electrode in 0.1 M $HClO_4$ solutions containing different isopropanol concentrations. The two first scans are shown, and the arrows indicate the scan number and direction. The vertical dashed lines show the position of the spikes related to the OH adsorption in the pure $HClO_4$ solution and in the presence of 0.001 M isopropanol. Scan rate: 50 mV s^{-1}.

the isopropanol oxidation reaction was studied on different single-crystal model electrodes and solution compositions. Fig. 1 shows the voltammograms obtained in perchloric acid solutions for different isopropanol compositions on the Pt(111) electrode. For the lowest tested concentration, 0.001 M (Fig. 1, bottom panel), the onset of the oxidation coincides with the onset of OH adsorption. On this electrode, the voltammetric signal appearing in 0.1 M $HClO_4$ between 0.5 and 0.8 V is linked to the OH adsorption. Also, a strong inhibition of the oxidation reaction is observed when the OH layer has been completed at 0.8 V. This behavior is similar to that reported for methanol and ethanol [18–20] where DFT calculations demonstrate that the presence of adsorbed OH on the surface facilitates the adsorption of the alcohol through the oxygen atom in a dehydrogenation process with a negligible kinetic barrier. Thus, the same mechanism is operating for the initial step of the isopropanol oxidation reaction: the adsorption of OH facilitates the oxidation reaction. The interaction of isopropanol with the surface in this potential region should be weak because the spikes at 0.8 V, which mark the completion of the OH adlayer, are still visible in both scan directions superimposed on the oxidation wave, implying that the OH adlayer formation is not significantly disturbed due to the presence of isopropanol in solution. Despite that, a shift in the position of the spikes to more positive potentials can be observed for 0.001 M isopropanol, as marked by the vertical lines in Fig. 1, indicating that the OH coverage is smaller than in pure perchloric solutions for the same potential. This shift suggests the consumption of adsorbed OH. It should be noted that OH adsorption/desorption is very fast, as revealed by the small dependence of the profile in this region with the scan rate up to 50 v s^{-1} [21], and if adsorbed OH is consumed during the reaction, the equilibrium situation is almost immediately restored.

The observation of the OH adsorption profile superimposed to the oxidation currents also means that the products or intermediates formed during oxidation do not interact with the surface. For instance, the oxidation of ethanol, which mainly produces acetic acid, shows a modification of this region due to the adsorption of acetate [19]. Moreover, the currents in the hydrogen adsorption region (below 0.4 V) in the presence of isopropanol are the same as those recorded in the supporting electrolyte (Fig. 1 and S1), a clear indication that no species originated from the oxidation of isopropanol are interacting with the surface. Thus, two possible oxidation products can be initially proposed that fulfill those conditions: CO_2 and acetone. Acetone does not interact with the Pt(111) surface, as the voltammetric profiles for this electrode in acetone-containing solutions demonstrate [3,4]. The formation of CO_2 can be discarded due to two facts: i) the production of CO_2 would imply the breaking of the C–C bonds with the formation of different fragments, which would generate several intermediates, such as CO and acetic acid, which are known to interact with the surface and ii) previous FTIR experiments show the formation of acetone in the whole potential region where the oxidation takes place and only traces of CO_2 are detected at potentials higher than 0.8 V [6,10–12]. Consequently, the isopropanol oxidation reaction on the Pt(111) electrode only yields acetone in a two-electron process. It should be noted that the currents for this oxidation reaction are significantly larger than those recorded for the C1–C2 alcohols. In fact, the shape of the voltammogram is the one typically expected for an irreversible process controlled by the diffusion of the reactant (isopropanol) and the decay in the current between the first and second scans is due to the depletion of isopropanol in the diffusion layer.

The qualitative behavior described for the 0.001 M isopropanol solution also holds for higher concentrations. No adsorbed species are detected on the electrode surface (Fig. 1 and S1), as revealed by the absence of modifications in the hydrogen adsorption profile. As the concentration increases the onset displaces to lower potential values, and for the highest concentration, the onset is ca. 0.3 V. It should be noted that adsorbed OH should be present on this electrode surface at potentials as low as 0.45 V on this electrolyte, just after the potential of zero total charge (pztc) [19,22]. For 0.01 M isopropanol, the currents are still controlled by diffusion, which implies a very high activity of the Pt(111) electrode for this reaction. The effective control by diffusion can be verified by analyzing the decay after the peak in the positive scan direction. The decay should be proportional to $(t\text{-}t_0)^{-1/2}$ after the appropriate t_0 has been selected [23,24]. As shown in Fig. S2, a perfect linear relationship is obtained when the currents after the peak are plotted vs. $(t\text{-}t_0)^{-1/2}$, with an intercept value of zero, within the error, which confirms the full control of the reaction by the diffusion of the reactants. Furthermore, for 0.1 M solutions, measured currents are so high that are severely affected by the ohmic drop in the electrolyte solution. The experimental curve was corrected after measuring the resistance for this solution using impedance (85 Ω), as shown in Fig. 1. The evolution of the current with the concentration of isopropanol allows obtaining the reaction order. To determine it, currents at 0.45 V, a potential where currents are not affected by diffusion limitations, are plotted vs. the isopropanol concentration. As can be seen in Fig. S3, the double logarithmic plot shows a linear relationship with a slope of 0.88, clearly showing that this is a first-order reaction for isopropanol.

To determine the activity of the electrode in absence of diffusion limitations, rotating disk experiments in the hanging meniscus configuration for 0.01 M isopropanol were carried out (Fig. 2A). As can be seen, typical curves are obtained in which the positive and negative scan directions are almost identical, indicating that the surface state in both directions is the same. Also, there is no significant diminution of the current upon cycling. As predicted by the Levich equation, which applies to diffusion-controlled processes, limiting current densities, j_{lim}, are proportional to the square root of the rotation rate (Fig. S4). From the curves in Fig. 2A, kinetic currents, j_k, can be calculated. For a first-order reaction, the total current can be written as:

$$\frac{1}{j} = \frac{1}{j_k} + \frac{1}{j_{\text{lim}}} \tag{1}$$

Solving for j_k, the following expression can be obtained:

$$j_k = \frac{j_{\text{lim}} j}{j_{\text{lim}} - j_k} \tag{2}$$

The logarithm of the kinetic currents vs. electrode potential was plotted in Fig. 2B for the curve at 900 rpm. Almost identical curves were obtained for the other rotation rates. As can be seen, two different Tafel slopes can be measured. Between 0.48 and 0.7 V, a very good linear relationship can be obtained, with a Tafel slope value of 72 ± 5 mV. A theoretical Tafel slope value of 59 mV is generally derived for mechanisms in which a chemical step after the first electron transfer is the rate-determining step (r.d.s.). Additionally, for lower potentials (between 0.4 and 0.46 V) a Tafel slope of ca. 129 mV is obtained, which implies that the first electron transfer is the r.d.s. The change of the Tafel slope is associated with a change in the mechanism, and this change occurs at ca. 0.47 V. This is the onset potential of adsorbed OH on this electrode as the difference between the calculated double layer currents and the voltammetric currents shows [19,22]. The change in mechanism is then related to the presence of adsorbed OH at E > 0.48 V. In the absence of OH, the formation of the adsorbed alkoxide is the r.d.s. according to:

$$Pt + CH_3CHOHCH_3 \rightarrow Pt - OCH(CH_3)_2 + H^+ + e^- \text{ r.d.s} \tag{3}$$

When OH is adsorbed on the surface, the reaction mechanism changes because adsorbed OH is involved in the mechanism as follows:

$$Pt + H_2O \rightleftharpoons Pt - OH + H^+ + e^- \tag{4}$$

$$Pt - OH + CH_3CHOHCH_3 \rightarrow Pt - OCH(CH_3)_2 + H_2O \text{ r.d.s} \tag{5}$$

This mechanism comprises the adsorption of OH in the first step, the formation of the adsorbed alkoxide by the reaction of adsorbed OH with an incoming isopropanol molecule in the r.d.s. For both mechanisms the final reaction is the dehydrogenation of the alpha carbon from the adsorbed alkoxide species to yield acetone:

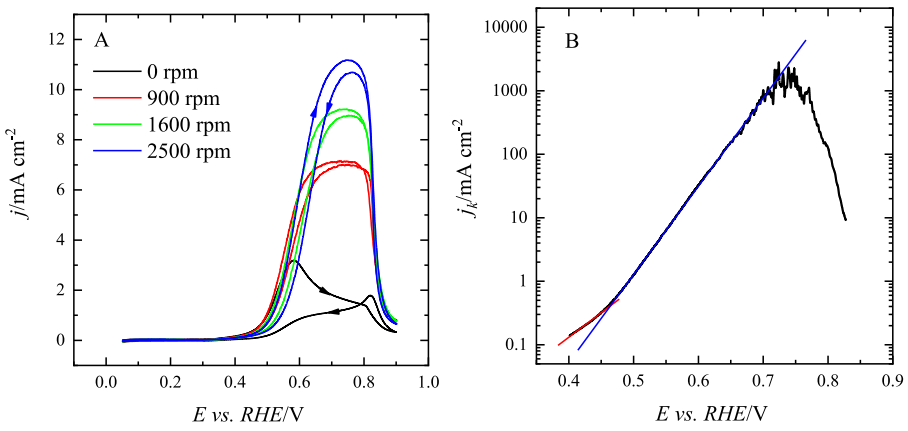

Fig. 2. A) Voltammetric profile for the Pt(111) electrode in 0.1 M $HClO_4$ + 0.01 M isopropanol solution under different rotation rates. Only the first scan is shown, and the arrows indicate the direction. Scan rate: 50 mV s^{-1}. B) Kinetic current obtained from the curve of panel A) at 900 rpm. The red and blue lines show the linear fitting obtained between 0.4 and 0.46 V, and 0.48 and 0.7 V, respectively. (For interpretation of the references to colour in this figure legend, the reader is referred to the Web version of this article.)

$$Pt - OCH(CH_3) \rightarrow Pt + CH_3COCH_3 + H^+ + e^- \quad (6)$$

It should be noted that DFT calculations indicate that the position of the hydrogen atom in this carbon is very close to the surface when the isopropanol molecule interacts with the Pt(111) through the oxygen [25]. In this position, the cleavage of the C–H bond should have a very small kinetic barrier, as has been already calculated for the oxidation of formic acid [26] or ethanol [19]. For a mechanism in which adsorbed species (i.e., Pt–OH) are involved in the first step before a chemical r.d.s., a theoretical value of the Tafel slope of 60 mV is expected in the potential region where the coverage of adsorbed OH is low, conditions that are achieved for E < 0.70 V. The excellent linearity of the logarithm plot between 0.48 and 0.7 V, support the proposed mechanism and the deviation from the value of 60 mV should be due to effects not considered in the equations, such as the surface charge or water structure, which may affect the kinetics.

If this mechanism is correct and the oxidation is facilitated by the presence of adsorbed OH on the surface, it is expected that the specific adsorption of sulfate should significantly diminish the currents. To verify this hypothesis, the oxidation of isopropanol was studied in 0.1 M H_2SO_4 (Fig. 3). On this electrode, sulfate adsorption starts at 0.3 V, and a well-ordered adlayer is achieved after the sharp spike at 0.49 V. When isopropanol is added, only significant currents are observed in the region where the sulfate adlayer has not been completed, i.e., below 0.48 V (Fig. S5). In fact, in the region below 0.4 V currents in sulfuric and perchloric acid solutions are very similar, indicating that the mechanism comprising reactions (3) and (6) is operating for these potentials. Although the sulfate adlayer on the Pt(111) electrode is open and includes water molecules [27], the formation of the ordered structure after the spike freezes the position of the different species on the adlayer and prevents the adsorption of OH. It should be noted that the formation of the ordered adlayer does not prevent species from interacting with the surface, as the oxygen reduction reaction demonstrates [28] In this case, the formation of the ordered sulfate structure inhibits the reaction due to the complete hindrance of the adsorption of OH.

Once the behavior and the mechanism of the reaction have been established for the Pt(111) electrode, the effect of the surface structure can be determined by studying the Pt(110) and Pt(100) electrodes. For the Pt(110) surface in perchloric acid (Fig. 4), currents are smaller than those measured for the Pt(111) electrode (Fig. S6), although, for 0.001 and 0.01 M isopropanol, diffusion control is also observed. For this reason, currents in the negative scan direction are smaller than those recorded in the positive direction, and the difference in the behavior between the first and second scan is then related to the depletion of isopropanol in the diffusion layer, as observed for the Pt(111) electrode. Also, at potentials higher than 0.8 V, the oxidation of isopropanol is strongly inhibited due to the irreversible transformation of adsorbed OH into oxides. It should be noted that the adsorption of OH on this electrode is expected at potentials higher than that of the pztc, which is located at 0.25 V [29,30], implying that the signals recorded in the blank voltammogram at potentials higher than this value correspond mainly to the adsorption of OH. Thus, the isopropanol oxidation reaction can proceed from that potential. However, although the onset potential for the reaction is lower than that measured for the Pt(111) electrode (Fig. S6), significant currents are only measured at E > 0.35 V. This fact indicates that the kinetics of the reaction between adsorbed OH and isopropanol are slower on the Pt(110) for a similar OH coverage. A possible explanation for this result relies on the formation of commensurate hexagonal water structures on the Pt(111) [31]. Those structures can easily incorporate adsorbed OH and transport it to the right location through a Grotthuss-like mechanism [20]. For this reason, traces of adsorbed OH on the Pt(111) surface can readily react with the incoming isopropanol molecule, whereas higher coverages are required for the same reaction rate on the Pt(110). For 0.1 M isopropanol, high currents are also measured, and, despite the high conductivity of the solution, peak currents are affected by ohmic drops.

Another difference in the behavior of the Pt(110) electrode with respect to that observed for the Pt(111) surface is the adsorption/oxidation of acetone. Acetone is adsorbed on this surface and is also reduced to isopropanol at potentials below 0.1 V [3,4]. In fact, the peak centered at 0.07 V observed in the negative scan direction (Fig. 4) is related to the reduction of acetone to isopropanol, although other minor products, such as propane, cannot be discarded [32]. On the other hand, when the behavior of acetone has been studied on this electrode, it has been observed that acetone-related species are adsorbed on the electrode surface, partially blocking hydrogen adsorption [3,4]. In this case, the inhibition of hydrogen adsorption at low potentials is small, indicating that the surface concentration of acetone is not very high because it diffuses from the surface to the bulk due to the concentration gradient. The partial blockage of the surface also explains the smaller currents measured for the Pt(110) electrode in comparison with the Pt(111) surface. For 0.001 M isopropanol solutions, peak currents for both electrodes are the same, within the reproducibility of the measurements, and the only significant difference is the lower onset potential for the Pt (110) electrode. For this concentration, the amount of produced acetone should be very low, and, as the voltammogram in Fig. 4 shows, the blockage of the hydrogen adsorption is almost negligible. As the isopropanol concentration increases, additional surface sites on the Pt(110) electrode are occupied by acetone-related species, resulting in lower-than-expected currents due to partial inhibition of the reaction and a larger difference between the currents for the Pt(111) and the Pt (110) electrodes.

The formation of acetone in the voltammogram can be followed by the reduction peak observed at 0.07 V. For that, the first voltammetric cycle for a freshly annealed Pt(110) electrode in 0.001 M isopropanol solution with different upper potential limits was recorded (Fig. S7). As

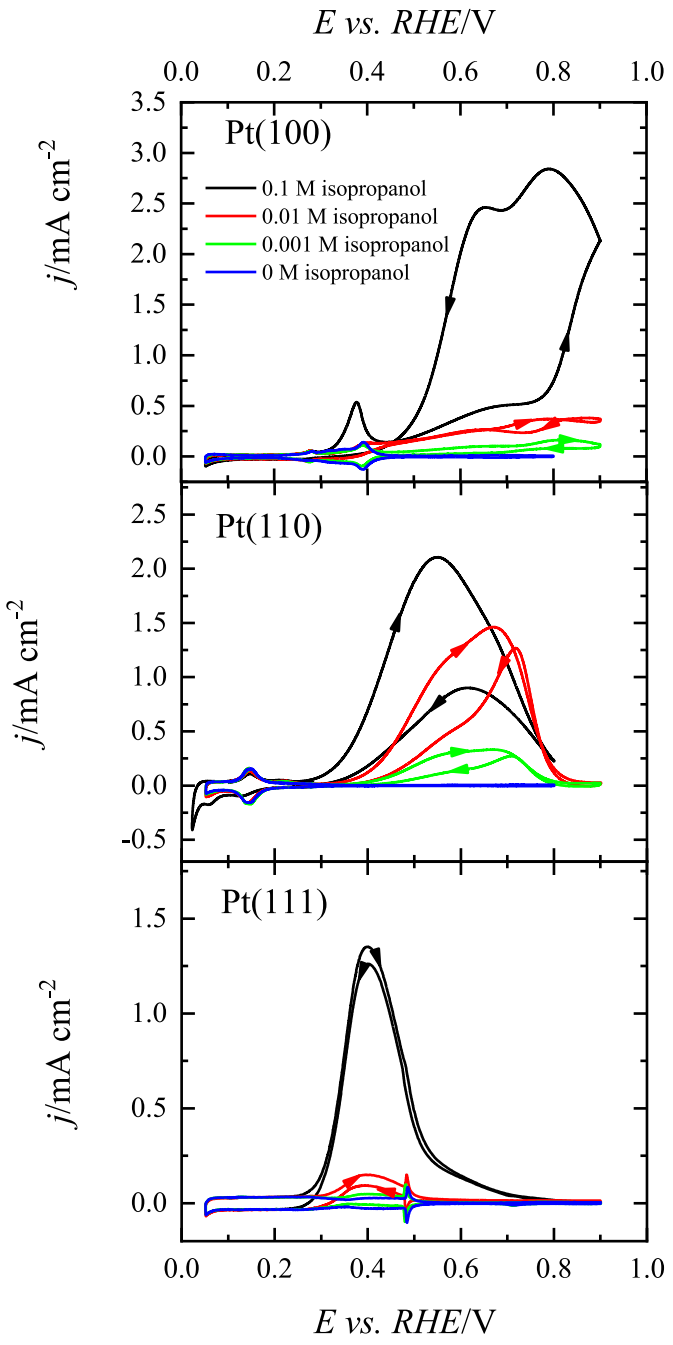

Fig. 3. Voltammetric profiles for the different low-index electrodes in 0.1 M H_2SO_4 solutions containing different isopropanol concentrations. Only the first scan is shown, and the arrows indicate the scan direction. Scan rate: 50 mV s^{-1}.

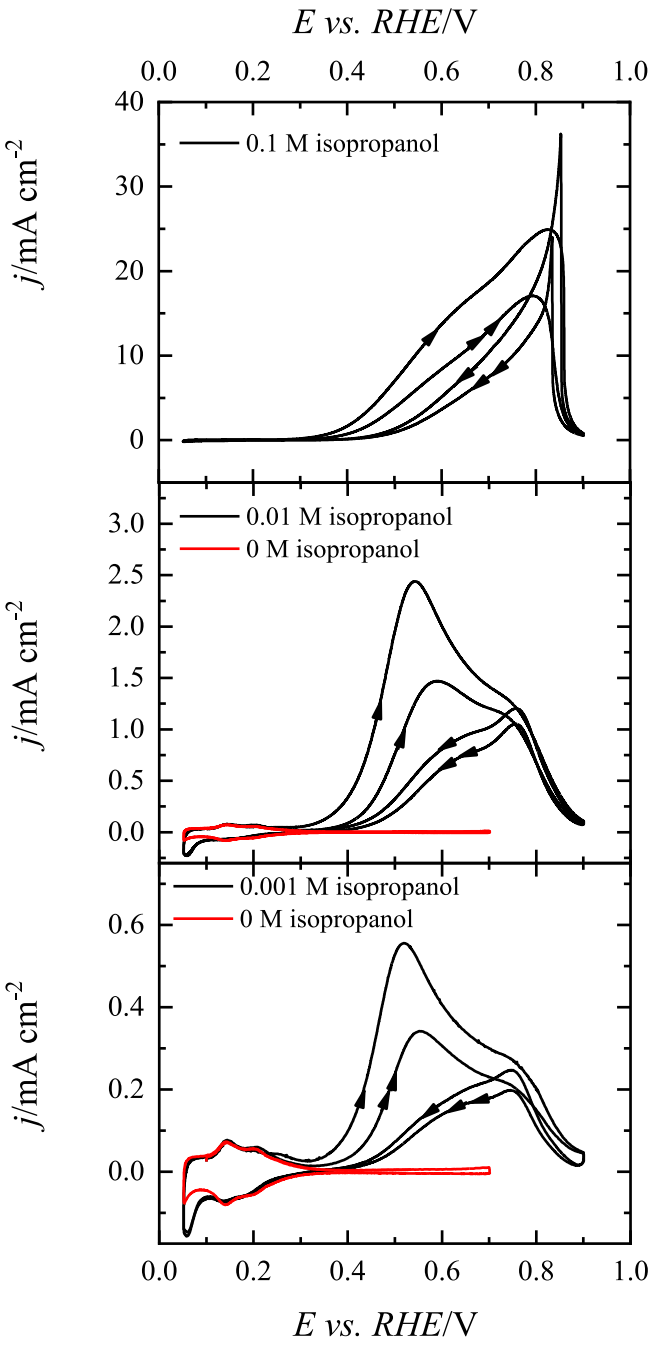

Fig. 4. Voltammetric profiles for the Pt(110) electrode in 0.1 M $HClO_4$ solutions containing different isopropanol concentrations. The two first scans are shown and the arrows indicate the scan number and direction. Scan rate: 50 mV s^{-1}.

can be seen, a progressive increase in the current at 0.07 V is observed as the upper potential limit increases from 0.3 V (where no significant oxidation current for isopropanol is observed) up to 0.8 V. This fact clearly indicates that the formation of acetone takes place in the whole potential range where isopropanol is oxidized. Moreover, the evolution of the voltammogram with the upper limit is that expected for a diffusion-controlled irreversible process, suggesting that no other product is formed. On the other hand, the presence of sulfate in the solution leads to a significant diminution of the currents and the displacement of the onset potentials to higher values due to the specific adsorption of sulfate (Fig. 3). In this case, owing to the open structure of the surface atoms of the Pt(110) electrode, the full sulfate adlayer does not block completely the oxidation of isopropanol unlike what is observed for the Pt(111) electrode, and some currents are recorded at high potential values.

The behavior of the Pt(100) electrode for the oxidation of alcohols and derived molecules presents some singularities with respect to the other basal planes since it is the most active for the cleavage of C–C bonds, as observed in the oxidation of ethanol or acetone [3,4,19,33]. In all these cases, this specific reactivity leads to the formation of adsorbed CO as soon as OH is adsorbed on the surface, that is, above 0.4 V. Adsorbed CO blocks the surface for the oxidation and it is oxidized in a sharp peak at ca. 0.75 V, restoring the initial activity on the surface. For this reason, when CO is formed at E > 0.4 V in the positive scan

direction, currents in the negative scan direction are higher than those recorded in the positive direction. For 0.001 M solution, the voltammogram does not show the typical shape associated with the formation of CO (Fig. 5). In fact, it is very similar to that recorded for the Pt(111) and Pt(110) electrodes with the same isopropanol concentration (Fig. S6). The only differences are related to smaller currents and the presence of a peak at 0.8 V. Both facts are related to the adsorption of acetone formed as a result of the oxidation of isopropanol. In the initial scan for this isopropanol concentration, the profile is identical to that obtained in the absence of isopropanol up to 0.4 V, indicating that the hydrogen is the only specie adsorbed in this region. At 0.4 V, which is the onset for OH adsorption on this electrode, the oxidation of isopropanol begins yielding acetone. Acetone-related species are adsorbed on the electrode surface, resulting in lower-than-expected currents and the oxidation peak at 0.8 V, which is characteristic of the oxidation of adsorbed acetone-related species [3,4]. At 0.9 V, oxidation is inhibited due to the transformation of adsorbed OH into oxide, which is inactive for the oxidation of alcohols. In the negative scan direction, the reduction of the oxides leads to the reactivation of the surface. In the second scan, adsorbed species are present on the surface, as can be seen by the partial blockage of the hydrogen adsorption and the lower currents. The effect of the adsorbed acetone-related species on this surface can also be assessed in the comparison with the other basal planes (Fig. S6). Although the onset potential is the lowest, peak currents do not reach the values of the other two electrodes.

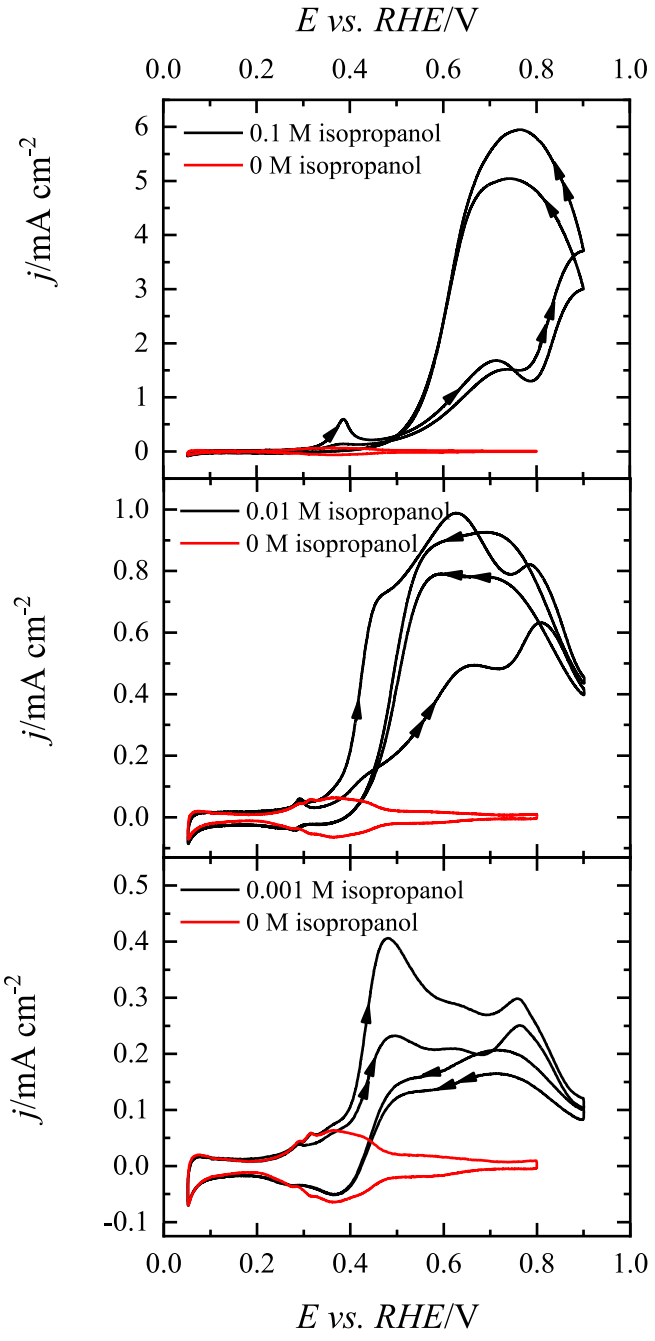

Fig. 5. Voltammetric profiles for the Pt(100) electrode in 0.1 M $HClO_4$ solutions containing different isopropanol concentrations. The two first scans are shown, and the arrows indicate the scan number and direction. Scan rate: 50 mV s^{-1}.

Increasing the concentration of isopropanol in the solution intensifies the effect of the adsorbed acetone species in the voltammetric behavior. For the 0.01 M isopropanol concentration, the initial behavior is similar to that observed for the 0.001 M concentration, but in the second scan, significant differences are already observed. Currents in this second scan are significantly smaller which implies that the surface is strongly blocked by the presence of acetone-related species formed during the first scan. Additionally, for the highest isopropanol concentration (0.1 M), important changes in the behavior are observed, especially during the first cycle. For this concentration, a peak at 0.4 V in the first scan is observed (Fig. 5 and S8), which is related to the cleavage of the C–C bond and the formation of adsorbed CO, as the experiments with ethanol demonstrated [19]. Due to the presence of adsorbed CO, which blocks the surface, currents in the positive scan direction are low until CO is oxidized at potentials higher than 0.8 V, reestablishing the activity of the surface. In the second positive scan, this peak is not observed because CO has been already formed in the negative scan direction between 0.6 and 0.4 V, as observed for ethanol or acetone [4,19]. Thus, for this surface, the cleavage of the C–C bond to yield adsorbed CO and eventually CO_2 is a minor path, although, at high concentrations, this minor path controls the kinetics of the isopropanol oxidation. This type of behavior in which a minor path leading to the formation of adsorbed CO controls the overall reactivity of the electrode has been already observed for other reactions, such as formic acid oxidation [18,26]. Again, the presence of sulfate in solutions leads to a significant diminution of the currents (Fig. 3), associated with the hindrance of OH adsorption.

Having established the behavior of the basal planes, the behavior of the stepped surfaces having (111) terraces and monoatomic (110) or (100) steps was studied (Fig. 6) to determine the influence of the step symmetry and terrace length on the reactivity. It should be highlighted that step sites are formed by atoms with a low coordination number and have a similar behavior that defects on surfaces. As a general trend for both stepped surface series, the onset for the isopropanol oxidation reaction moves to higher potential values as the step density increases. This shift follows the behavior of OH adsorption on the terraces which also shifts to higher values as the step density increases [34]. On the other hand, adsorbed OH on the steps, which occurs at potentials positive to the characteristic peak for the step sites (0.13 V and 0.32 V for the (110) and (100) steps, respectively) [35] seems to be unreactive for the oxidation of isopropanol because no oxidation current is observed after the peaks. In fact, the signals for the H/OH adsorption on the peaks are still observed in the presence of isopropanol, which indicates that no species derived from isopropanol are adsorbed on the step sites. Aside from these changes, the only electrode whose behavior is significantly different is the Pt(311), which is the turning point in the series and can be considered as a stepped surface having 2 atom-wide (111) terraces and a monoatomic (100) step or 2 atom-wide (100) terraces with a (111) monoatomic step. For this reason, it has the combined characteristics of the (111) and (100) planes.

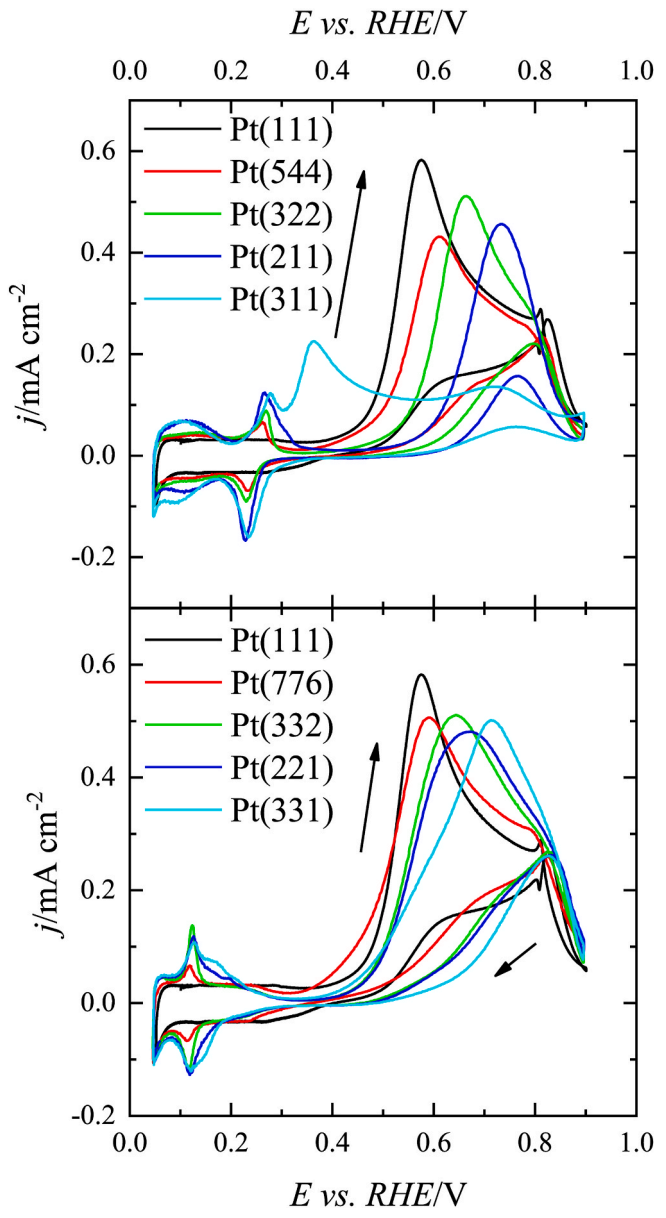

Fig. 6. Voltammetric profiles for the stepped electrode having (111) terraces and monoatomic (100) steps (upper panel) and (110) steps (lower panel) electrode in 0.1 M $HClO_4$ + 0.001 M isopropanol. Only the first scan is shown, and the arrows indicate the scan direction. Scan rate: 50 mV s^{-1}.

3.2. FTIR results for the isopropanol oxidation reaction

According to the observed electrochemical behavior, isopropanol oxidation will produce only acetone on the Pt(111) electrode. On the Pt (110) surface, acetone-related species will be adsorbed on the surface, partially inhibiting the oxidation reaction, whereas the Pt(100) electrode is the only one able to break the C–C chain resulting in adsorbed CO, which eventually is oxidized to CO_2. For this latter surface, the adsorption of different species formed during the oxidation process is important, because it shows the largest inhibition. To corroborate these hypotheses, FTIR experiments were conducted. Fig. 7 shows the spectra obtained for the different electrodes as a function of the electrode potential in 0.1 M $HClO_4$ + 0.1 M isopropanol, using the spectrum taken at 0.1 V as reference. The initially expected bands are those related to the consumption of isopropanol, the formation of acetone, and, if the C–C bond is cleaved, adsorbed CO and solution CO_2. The frequencies and the band assignment for those species are listed in Table 1 [8,10,12,36,37].

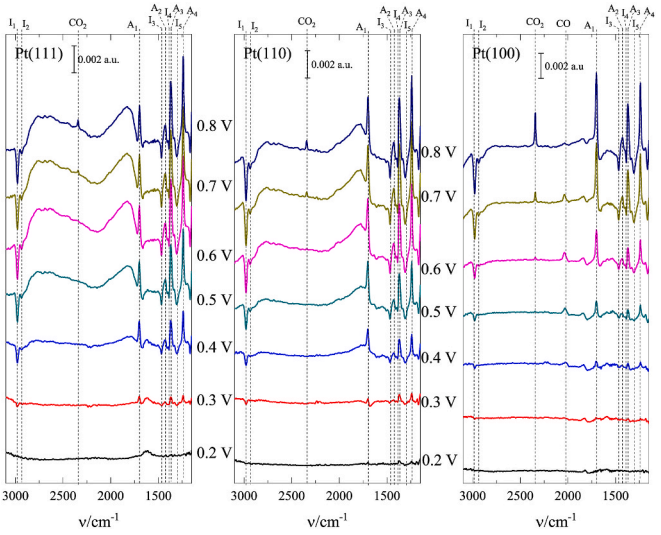

Fig. 7. FTIR spectra as a function of the electrode potential for the oxidation of isopropanol on the low index planes of Pt in 0.1 M $HClO_4$ + 0.1 M isopropanol. The reference spectrum is taken at 0.1 V.

Table 1
Vibrational modes and frequencies for the FTIR spectra of acetone, isopropanol, adsorbed CO on Pt, and CO_2.

	Mode	Frequency	Name	Refs.
Acetone	ν (CO)	1697 cm^{-1}	A_1	[12,
	δ (CH_3)	1436-1420 cm^{-1}	A_2	36–38]
	δ_{sym} (CH_3)/ν_{asym}(C–C)	1367 cm^{-1}	A_3	
	ν_{asym} (C–C)	1238 cm^{-1}	A_4	
Isopropanol	ν (CH)	2937 cm^{-1}	I_1	[8,12,38]
	ν (CO)	2881 cm^{-1}	I_2	
	δ_{asym} (CH_3)/δ_{sym} (CH_3)	1466 cm^{-1}	I_3	
	ν (C–C)	1384 cm^{-1}	I_4	
	δ (OH)	1308 cm^{-1}	I_5	
Adsorbed CO	ν (CO)	2020–2050 cm^{-1}	CO	
CO_2	ν (OCO)	2349 cm^{-1}	CO_2	

As can be seen in Fig. 7 for the oxidation of 0.1 M isopropanol on the Pt (111) electrode, acetone-related bands start to develop from 0.4 V, which is the onset of the oxidation of isopropanol. From this potential value, acetone bands start to grow in parallel with the appearance of the negative bands related to the consumption of isopropanol. Moreover, the relative intensity of the different bands for acetone and isopropanol are the same as those observed in the reference spectrum, which clearly indicates that the main product of the oxidation of isopropanol is acetone. It should be noted that a small CO_2 band is observed at E > 0.7 V, which has not been previously reported for the Pt(111) electrode [8, 10]. The presence of a small amount of CO_2 indicates that the C–C bond has been broken. The cleavage of the C–C bond in isopropanol implies the formation of different fragments that can absorb on the surface. However, the voltammetric profile in Fig. 1 and S1 clearly shows the absence of any adsorbed species on the electrode because the hydrogen profile has not been altered. Thus, the presence of this small amount of CO_2 must be related to the presence of defects on the Pt(111) electrode employed in the FTIR experiments. The electrodes used in the FTIR experiments are larger than those used in voltammetry and the use of the thin film configuration causes additional damage to the electrode surface, so the number of defects in this electrode is higher than the one used in voltammetry. For the Pt(110) electrode, the spectra are very similar to that of the Pt(111). The only significant differences are observed for the Pt(100) surface, because, in this case, the band related

to linearly adsorbed CO is observed at E > 0.4 V, coinciding with the signals observed in Fig. S8, and confirming that this signal during the first scan is related to the cleavage of the C–C band leading to the formation of adsorbed CO. At E = 0.6 V, the intensity of this band starts to diminish, and, in parallel, the CO_2 band emerges as the result of the oxidation of adsorbed CO.

The FTIR spectra at 0.1 M isopropanol are dominated by the large amount of acetone produced during oxidation. Any other species or adsorbate formed from the oxidation, except for adsorbed CO and CO_2, are expected to have bands in the same regions as acetone and isopropanol. The high-intensity bands observed for acetone and isopropanol prevent the observation of any other species that may have formed during the oxidation. In an attempt to detect additional species, 0.01 M isopropanol in perchloric acid was used for acquiring a new set of spectra (Fig. 8). As can be seen, for this concentration, bands for acetone are smaller, but still clearly visible, while the negative bands related to the consumption of isopropanol have almost disappeared. Despite that, for the Pt(111) and Pt(110) electrodes, no new features can be observed in the spectra in comparison to that obtained for 0.1 M isopropanol and the bands for acetone have the expected shape and intensity of the reference samples [8,10,12,36,37]. On the other hand, for the Pt(100) electrode, some differences can be observed. Again, a small band related to the formation of adsorbed CO can be detected at E > 0.4 V. Additionally, some changes in the region between around 1400 cm^{-1} are observed. Acetone spectra show two δ (CH_3) bands at 1420 and 1436 cm^{-1} [10], whose intensity are smaller than the combination band δ_{sym} (CH_3)/ν_{asym}(C–C) at 1367 cm^{-1} [10]. For this electrode, at E > 0.5 V a new band at 1406 cm^{-1} starts to appear, and eventually, at E = 0.8 V, this band is larger than that at 1367 cm^{-1}. Clearly, a new species is formed at a potential that is close to the appearance of adsorbed CO. Thus, the species should be related to the C–C bond breaking. Carboxylic acids adsorb on platinum as carboxylates in a bidentate form with the two oxygen atoms bond to the surface [39]. Band frequencies for these adsorbed species are around 1400-1410 cm^{-1}. Thus, it can be proposed that the cleavage of the C–C chain will initially produce two fragments on the Pt(100) electrode: $\cdot CH_3$ and $\cdot COCH_3$ at E > 0.4 V. The adsorbed $\cdot COCH_3$ fragment has been also proposed in the oxidation of ethanol [19,40–42] and has two possible evolutions: i) the C–C bond brakes again producing adsorbed CO and an additional $\cdot CH_3$ fragment or ii) it is oxidized to acetic acid, which can be adsorbed on the surface as acetate in a bidentate configuration. As shown also for ethanol oxidation, $\cdot CH_3$ fragments are also oxidized to adsorbed CO and, at higher potentials, to CO_2 [40,41] or can be reduced to CH_4 at potentials close to hydrogen evolution [43,44].

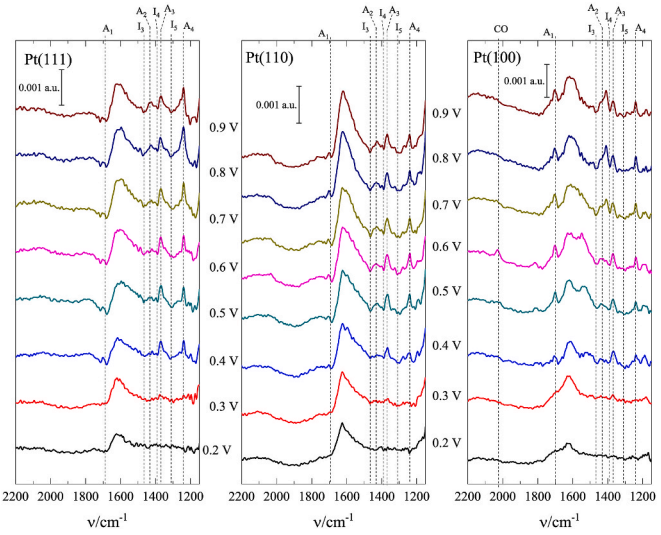

Fig. 8. FTIR spectra as a function of the electrode potential for the oxidation of isopropanol on the low index planes of Pt in 0.1 M $HClO_4$ + 0.01 M isopropanol. The reference spectrum is taken at 0.1 V.

4. Conclusions

Isopropanol oxidation on platinum is facilitated by the presence of adsorbed OH on the electrode surface because the reaction of adsorbed OH with the incoming alcohol molecule gives rise to the facile formation of the adsorbed alkoxide species. According to the kinetic parameters obtained for the reaction, this is the rate-determining step in the oxidation mechanism. As proposed by the voltammetric behavior and confirmed by the FTIR experiments, acetone is the only product formed on the Pt(111) and Pt(110) electrodes. Due to the negligible interaction of acetone with the Pt(111) electrode [3,4], the oxidation of isopropanol is a diffusion-controlled process for all the studied concentrations. For the Pt(110) electrode, acetone is adsorbed on the electrode surface and for this reason, currents are smaller than those on the Pt(111). Nevertheless, very high currents are obtained for 0.1 M isopropanol, and, for lower concentrations, currents are controlled by diffusion. Significantly lower currents are measured for the Pt(100) electrode due to two different facts: the stronger interaction of acetone with the surface and the cleavage of the C–C bond which results in the adsorption of CO and acetate. On the other hand, in absence of adsorbed species, that is for very low isopropanol concentrations, the onset of the oxidation follows the order Pt(100)<Pt(110)<Pt(111). This order is linked to the availability and reactivity of adsorbed OH on the surface. The opposite order is found for the peak currents and onset at high concentrations because, in this case, the reactivity is governed by the adsorbed species formed during the oxidation process. This fact reveals the importance of the adsorbed species in the oxidation mechanism. This study has also important consequences for practical applications. The significant dependence of the reactivity with the surface structure implies that the surface of the nanoparticles should be tailored so that the maximum activity is reached. For that, (111) domains in the nanoparticles should be maximized while reducing the ratio of (100) domains.

CRediT authorship contribution statement

Dalila S. Mekazni: Investigation, Formal analysis. **Rosa M. Arán-Ais:** Investigation, Formal analysis, Writing – review & editing. **Enrique Herrero:** Conceptualization, Formal analysis, Writing – original draft, Supervision. **Juan M. Feliu:** Formal analysis, Writing – review & editing, Supervision.

Declaration of competing interest

The authors declare that they have no known competing financial interests or personal relationships that could have appeared to influence the work reported in this paper.

Data availability

Data will be made available on request.

Acknowledgments

This research was funded by Ministerio de Ciencia e Innovación (Spain) grant number PID2019-105653 GB-I00) and Generalitat Valenciana (Spain) grant number PROMETEO/2020/063. RMAA acknowledges the financial support from Generalitat Valenciana (CDEIGENT/2019/018). DSM thanks the Government of Argelia for the award of a doctoral fellowship to support her studies at the University of Alicante.

Appendix A. Supplementary data

Supplementary data to this article can be found online at https://doi.org/10.1016/j.jpowsour.2022.232396.

References

[1] P. Preuster, C. Papp, P. Wasserscheid, Liquid organic hydrogen carriers (LOHCs): toward a hydrogen-free hydrogen economy, Acc. Chem. Res. 50 (2017) 74–85, https://doi.org/10.1021/acs.accounts.6b00474.

[2] M. Brodt, K. Müller, J. Kerres, I. Katsounaros, K. Mayrhofer, P. Preuster, P. Wasserscheid, S. Thiele, The 2-propanol fuel cell: a review from the perspective of a hydrogen energy economy, Energy Technol. 9 (2021), 2100164, https://doi.org/10.1002/ENTE.202100164.

[3] C.J. Bondue, Z. Liang, M.T.M. Koper, Dissociative adsorption of acetone on platinum single-crystal electrodes, J. Phys. Chem. C 125 (2021) 6643–6649, https://doi.org/10.1021/acs.jpcc.0c11360.

[4] D.S. Mekazni, R.M. Arán-Ais, J.M. Feliu, E. Herrero, Understanding the electrochemical hydrogenation of acetone on Pt single crystal electrodes, J. Electroanal. Chem. 922 (2022), 116697, https://doi.org/10.1016/J.JELECHEM.2022.116697.

[5] P. Hauenstein, D. Seeberger, P. Wasserscheid, S. Thiele, High performance direct organic fuel cell using the acetone/isopropanol liquid organic hydrogen carrier system, Electrochem. Commun. 118 (2020), 106786, https://doi.org/10.1016/j.elecom.2020.106786.

[6] S.G. Sun, D.F. Yang, Z.W. Tian, In situ FTIR studies on the adsorption and oxidation of n-propanol and isopropanol at a platinum electrode in sulphuric acid solutions, J. Electroanal. Chem. Interfacial Electrochem. 289 (1990) 177–187, https://doi.org/10.1016/0022-0728(90)87215-6.

[7] S.G. Sun, Y. Lin, In situ FTIR spectroscopic investigations of reaction mechanism of isopropanol oxidation on platinum single crystal electrodes, Electrochim. Acta 41 (1996) 693–700, https://doi.org/10.1016/0013-4686(95)00358-4.

[8] A. Santasalo, F.J. Vidal-Iglesias, J. Solla-Gullón, A. Berná, T. Kallio, J.M. Feliu, Electrooxidation of methanol and 2-propanol mixtures at platinum single crystal electrodes, Electrochim. Acta 54 (2009) 6576–6583, https://doi.org/10.1016/j.electacta.2009.06.033.

[9] P. Khanipour, S. Haschke, J. Bachmann, K.J.J. Mayrhofer, I. Katsounaros, Electrooxidation of saturated C1-C3 primary alcohols on platinum: potential-resolved product analysis with electrochemical real-time mass spectrometry (EC-RTMS), Electrochim. Acta 315 (2019) 67–74, https://doi.org/10.1016/j.electacta.2019.05.070.

[10] F. Waidhas, S. Haschke, P. Khanipour, L. Fromm, A. Görling, J. Bachmann, I. Katsounaros, K.J.J. Mayrhofer, O. Brummel, J. Libuda, Secondary alcohols as rechargeable electrofuels: electrooxidation of isopropyl alcohol at Pt electrodes, ACS Catal. (2020) 6831–6842, https://doi.org/10.1021/acscatal.0c00818.

[11] S.G. Sun, Y. Lin, Kinetics of isopropanol oxidation on Pt(111), Pt(110), Pt(100), Pt (610) and Pt(211) single crystal electrodes -: studies of in situ time-resolved FTIR spectroscopy, Electrochim. Acta 44 (1998) 1153–1162, https://doi.org/10.1016/S0013-4686(98)00218-7.

[12] E. Pastor, S. González, A.J. Arvia, Electroreactivity of isopropanol on platinum in acids studied by DEMS and FTIRS, J. Electroanal. Chem. 395 (1995) 233–242, https://doi.org/10.1016/0022-0728(95)04129-C.

[13] J. Schnaidt, Z. Jusys, R.J. Behm, Electrooxidation of 1-propanol on Pt - mechanistic insights from a spectro-electrochemical study using isotope labeling, J. Phys. Chem. C 116 (2012) 25852–25867, https://doi.org/10.1021/jp3086733.

[14] J. Schnaidt, M. Heinen, Z. Jusys, R.J. Behm, Oxidation of 1-propanol on a Pt film electrode studied by combined electrochemical, in situ IR spectroscopy and online mass spectrometry measurements, Electrochim. Acta 104 (2013) 505–517, https://doi.org/10.1016/J.ELECTACTA.2012.12.139.

[15] E. Pastor, S. Wasmus, T. Iwasita, M.C. Arévalo, S. González, A.J. Arvia, Spectroscopic investigations of C3 primary alcohols on platinum electrodes in acid solutions.: Part I. n-propanol, J. Electroanal. Chem. 350 (1993) 97–116, https://doi.org/10.1016/0022-0728(93)80199-R.

[16] J. Clavilier, D. Armand, S.G. Sun, M. Petit, Electrochemical adsorption behaviour of platinum stepped surfaces in sulphuric acid solutions, J. Electroanal. Chem. Interfacial Electrochem. 205 (1986) 267–277, https://doi.org/10.1016/0022-0728(86)90237-8.

[17] E. Herrero, J.M. Orts, A. Aldaz, J.M. Feliu, Scanning tunneling microscopy and electrochemical study of the surface structure of Pt(10,10,9) and Pt(11,10,10) electrodes prepared under different cooling conditions, Surf. Sci. 440 (1999) 259–270, https://doi.org/10.1016/S0039-6028(99)00813-4.

[18] R. Rizo, R.M. Arán-Ais, E. Herrero, On the oxidation mechanism of C1-C2 organic molecules on platinum. A comparative analysis, Curr. Opin Electrochem. 25 (2021), 100648, https://doi.org/10.1016/J.COELEC.2020.100648.

[19] R. Rizo, A. Ferre-Vilaplana, E. Herrero, J.M. Feliu, Ethanol electro-oxidation reaction selectivity on platinum in aqueous media, ACS Sustain. Chem. Eng. (2022), https://doi.org/10.1021/ACSSUSCHEMENG.2C02663.

[20] D.S. Mekazni, R.M. Arán-Ais, A. Ferre-Vilaplana, E. Herrero, Why methanol electro-oxidation on platinum in water takes place only in the presence of adsorbed OH, ACS Catal. 12 (2022) 1965–1970, https://doi.org/10.1021/ACSCATAL.1C05122/ASSET/IMAGES/LARGE/CS1C05122_0005.JPEG.

[21] C.A.C.A. Angelucci, E. Herrero, J.M.J.M. Feliu, Modeling CO oxidation on Pt(111) electrodes, J. Phys. Chem. C 114 (2010) 14154–14163, https://doi.org/10.1021/jp103597w.

[22] N. Garcia-Araez, V. Climent, E. Herrero, J.M.M. Feliu, J. Lipkowski, Thermodynamic approach to the double layer capacity of a Pt(1 1 1) electrode in perchloric acid solutions, Electrochim. Acta 51 (2006) 3787–3793, https://doi.org/10.1016/j.electacta.2005.10.043.

[23] E. Vallés, E. Gómez, J.M. Feliu, A. Aldaz, Oxidation of mesoxalate on gold in basic media, J. Electroanal. Chem. 190 (1985) 95–101, https://doi.org/10.1016/0022-0728(85)80079-6.

[24] G. Bontempelli, S. Daniele, F. Magno, Simple relationship for calculating backward to forward peak-current ratios in cyclic voltammetry, Anal. Chem. 57 (1985) 1503–1504, https://doi.org/10.1021/AC00284A081.

[25] P.C.D. Mendes, R. Costa-Amaral, J.F. Gomes, J.L.F. da Silva, The influence of hydroxy groups on the adsorption of three-carbon alcohols on Ni(111), Pd(111) and Pt(111) surfaces: a density functional theory study within the D3 dispersion correction, Phys. Chem. Chem. Phys. 21 (2019) 8434–8444, https://doi.org/10.1039/C9CP00752K.

[26] A. Ferre-Vilaplana, J.V.v. Perales-Rondón, C. Buso-Rogero, J.M.M. Feliu, E. Herrero, Formic acid oxidation on platinum electrodes: a detailed mechanism supported by experiments and calculations on well-defined surfaces, J. Mater. Chem. A. 5 (2017) 21773–21784, https://doi.org/10.1039/C7TA07116G.

[27] A.M. Funtikov, U. Linke, U. Stimming, R. Vogel, An in-situ STM study of anion adsorption on Pt(111) from sulfuric acid solutions, Surf. Sci. 324 (1995) L343–L348, https://doi.org/10.1016/0039-6028(94)00774-8.

[28] M.D. Maciá, J.M. Campiña, E. Herrero, J.M. Feliu, On the kinetics of oxygen reduction on platinum stepped surfaces in acidic media, J. Electroanal. Chem. 564 (2004) 141–150, https://doi.org/10.1016/j.jelechem.2003.09.035.

[29] N. Garcia-Araez, V. Climent, J. Feliu, Potential-dependent water orientation on Pt (111), Pt(100), and Pt(110), as inferred from laser-pulsed experiments. Electrostatic and chemical effects, J. Phys. Chem. C 113 (2009) 9290–9304, https://doi.org/10.1021/jp900792q.

[30] J. Clavilier, R. Albalat, R. Gomez, J.M. Orts, J.M. Feliu, A. Aldaz, Study of the charge displacement at constant potential during CO adsorption on Pt(110) and Pt (111) electrodes in contact with a perchloric acid solution, J. Electroanal. Chem. 330 (1992) 489–497, https://doi.org/10.1016/0022-0728(92)80326-Y.

[31] K. Raghavan, K. Foster, M. Berkowitz, Comparison of the structure and dynamics of water at the Pt(111) and Pt(100) interfaces: molecular dynamics study, Chem. Phys. Lett. 177 (1991) 426–432, https://doi.org/10.1016/0009-2614(91)85078-B.

[32] C.J. Bondue, F. Calle-Vallejo, M.C. Figueiredo, M.T.M. Koper, Structural principles to steer the selectivity of the electrocatalytic reduction of aliphatic ketones on platinum, 2, Nature Catalysis 2 (3) (2019) 243–250, https://doi.org/10.1038/s41929-019-0229-3, 2019.

[33] R. Rizo, S. Pérez-Rodríguez, G. García, Well-Defined platinum surfaces for the ethanol oxidation reaction, Chemelectrochem 6 (2019) 4725–4738, https://doi.org/10.1002/celc.201900600.

[34] J. Clavilier, A. Rodes, K. el Achi, M. Zamakhchari, Electrochemistry at platinum single crystal surfaces in acidic media : hydrogen and oxygen adsorption, J. de Chimie Physique 88 (1991) 1291–1337, https://doi.org/10.1051/jcp/1991881291.

[35] R. Rizo, J. Fernández-Vidal, L.J. Hardwick, G.A. Attard, F.J. Vidal-Iglesias, V. Climent, E. Herrero, J.M. Feliu, Investigating the presence of adsorbed species on Pt steps at low potentials, Nat. Commun. 13 (2022), https://doi.org/10.1038/s41467-022-30241-7.

[36] J.J. Max, C. Chapados, Infrared spectroscopy of acetone–water liquid mixtures. I. Factor analysis, J. Chem. Phys. 119 (2003) 5632, https://doi.org/10.1063/1.1600438.

[37] J.J. Max, C. Chapados, Infrared spectroscopy of acetone–water liquid mixtures. II. Molecular model, J. Chem. Phys. 120 (2004) 6625, https://doi.org/10.1063/1.1649936.

[38] F. Waidhas, S. Haschke, P. Khanipour, L. Fromm, A. Görling, J. Bachmann, I. Katsounaros, K.J.J. Mayrhofer, O. Brummel, J. Libuda, Secondary alcohols as rechargeable electrofuels: electrooxidation of isopropyl alcohol at Pt electrodes, ACS Catal. 10 (2020) 6831–6842, https://doi.org/10.1021/acscatal.0c00818.

[39] A. Rodes, E. Pastor, T. Iwasita, An ftir study on the adsorption of acetate at the basal planes of platinum single-crystal electrodes, J. Electroanal. Chem. 376 (1994) 109–118, https://doi.org/10.1016/0022-0728(94)03585-7.

[40] V. del Colle, J. Souza-Garcia, G. Tremiliosi-Filho, E. Herrero, J.M. Feliu, Electrochemical and spectroscopic studies of ethanol oxidation on Pt stepped surfaces modified by tin adatoms, Phys. Chem. Chem. Phys. 13 (2011) 12163–12172, https://doi.org/10.1039/c1cp20546c.

[41] J. Souza-Garcia, E. Herrero, J.M. Feliu, Breaking the C-C bond in the ethanol oxidation reaction on platinum electrodes: effect of steps and ruthenium adatoms, ChemPhysChem 11 (2010) 1391–1394, https://doi.org/10.1002/cphc.201000139.

[42] F. Colmati, G. Tremiliosi-Filho, E.R. Gonzalez, A. Berná, E. Herrero, J.M. Feliu, Surface structure effects on the electrochemical oxidation of ethanol on platinum single crystal electrodes, Faraday Discuss 140 (2008) 379–397, https://doi.org/10.1039/b802160k, discussion 417-37.

[43] U. Schmiemann, U. Müller, H. Baltruschat, The influence of the surface structure on the adsorption of ethene, ethanol and cyclohexene as studied by DEMS, Electrochim. Acta 40 (1995) 99–107, https://doi.org/10.1016/0013-4686(94)00243-T.

[44] B. Bittins-Cattaneo, S. Wilhelm, E. Cattaneo, H.W. Buschmann, W. Vielstich, Intermediates and products of ethanol oxidation on platinum in acid solution, Ber. Bunsen Ges. Phys. Chem. 92 (1988) 1210–1218, https://doi.org/10.1002/bbpc.198800300.